ELSEVIER

Journal of Magnetism and Magnetic Materials 172 (1997) 53–60

Journal of magnetism and magnetic materials

A unified theory of CIP and CPP giant magnetoresistance in magnetic sandwiches

A. Vedyayev[a,*], M. Chshiev[a], N. Ryzhanova[a], B. Dieny[b], C. Cowache[b], F. Brouers[c]

[a] *Department of Physics, Moscow Lomonosov University, Moscow, 119899, Russia*
[b] *CEA/Grenoble, Departement de Recherche Fondamentale sur la Matière Condensée, SP2M/NM, 38054 Grenoble, France*
[c] *Etude physique de Materiaux, Institut de Physique, Sart Tilman, Liege 4000, Belgium*

Received 18 February 1997

Abstract

A theory of giant magnetoresistance (GMR) in magnetic sandwiches F/P/F for current in plane (CIP) and current perpendicular to plane (CPP) geometries is developed. We adopted the free electron model described by four parameters: mean free paths and scattering amplitudes (coherent potentials) at the interfaces for spin-up and spin-down electrons. For both CIP and CPP geometries, we calculated the conductivities and GMR using Kubo formalism and the Green function technique in mixed real space–momentum representation. The final expressions for GMR in both geometries were obtained using the same microscopic parameters. Main attention was paid to the relative role of spin-dependent bulk and interfacial scattering. It was shown that increasing of surface scattering for fixed spin asymmetry leads to non-monotonic behaviour of CIP GMR due to renormalization of the scattering amplitude. In the case of CPP geometry the dependence of GMR on interfacial scattering amplitude is monotonic.

Keywords: Magnetic multilayers; Giant magnetoresistance

PACS: 75.50C; 72.15C; 75.50R

1. Introduction

Since the discovery of the giant magnetoresistance (GMR) in Fe/Cr multilayers [1, 2] and observation of this effect in many structures (multilayers or sandwiches F/P/F, where F is the ferromagnetic layer and P the non-magnetic spacer) [3] the problem of relative importance of spin-dependent electron scattering in the bulk or on the interfaces is widely discussed but until now the problem is not completely solved. Other interesting problem arises, when one consider two different geometries: current in plane (CIP) and current perpendicular to the plane (CPP). It appears that for CIP geometry, GMR is due to classical size effect and

* Corresponding author. Fax: + 7-095-932-8820; e-mail: vedy@vedy.phys.msu.su.

PII S0304-8853(97)00081-4

quasiexponentially decreases with the thickness of the paramagnetic layer [4–6]. For CPP geometry, the total resistivity of the system may be calculated like the sum of the weighted resistivities in series for each spin channel [7], if one does not take into account spin-flip processes [8] and spin-dependent potential barriers between layers [9]. However, there does not exist a theory, where the bulk and surface scattering are treated on the same footing for both geometries (CIP and CPP), so that the final expressions for CIP and CPP GMR would involve the same parameters of the model, unique for both geometries. In this paper we present the quantum statistical theory of GMR for both CIP and CPP geometries in the sandwich structure consisting of two ferromagnetic films, separated by metallic paramagnetic spacer with interfaces on the boundaries. For the calculation of the conductivity of the system we used Kubo formalism and the Green functions method.

2. Giant magnetoresistance in CPP geometry

The Kubo formula for CPP two-point conductivity $\sigma(z, z')$ may be written as follows [10]:

$$\sigma(z, z') = \frac{1}{\pi}\frac{e^2}{\hbar}\left(\frac{\hbar^2}{2m}\right)^2 \sum_{\kappa}\left\{\left[\frac{\partial G_\kappa}{\partial z} - \frac{\partial G_\kappa^*}{\partial z}\right]\left[\frac{\partial G_\kappa}{\partial z'} - \frac{\partial G_\kappa^*}{\partial z'}\right] - \left[\frac{\partial^2 G_\kappa}{\partial z \partial z'} - \frac{\partial^2 G_\kappa^*}{\partial z \partial z'}\right][G_\kappa - G_\kappa^*]\right\}, \tag{1}$$

where $G_\kappa \equiv G_\kappa(z, z')$ and $G_\kappa^* \equiv G_\kappa^*(z, z')$ are retarded and advanced Green functions of the system, κ the electron's momentum in XY-plane of the film, and z the direction perpendicular to the film's plane. The above expression (Eq. (1)) is exact if one knows the exact Green functions, but further we will use the expressions for the Green functions, averaged over the distribution of impurities in each XY-monolayer, so that each individual layer (i) is characterized by its own coherent potential $\Sigma_i^{\uparrow(\downarrow)}$, whose value for ferromagnetic layer depends on the electron's spin $\uparrow(\downarrow)$. The coherent potential is the solution of the equation

$$x_i \frac{\epsilon_i^{\mathrm{A}} - \Sigma_i}{1 - (\epsilon_i^{\mathrm{A}} - \Sigma_i)(1/N)\sum_\kappa G_\kappa(z, z)} + (1 - x_i)\frac{\epsilon_i^{\mathrm{B}} - \Sigma_i}{1 - (\epsilon_i^{\mathrm{B}} - \Sigma_i)(1/N)\sum_\kappa G_\kappa(z, z)} = 0$$

where we consider every layer i as an alloy $\mathrm{A}_{x_i}\mathrm{B}_{1-x_i}$ with random distribution of atoms type A(B) on the lattice sites, $\epsilon_i^{\mathrm{A(B)}}$ are the onsite matrix elements of the potential of A(B) atoms, $(1/N)\sum_\kappa G_\kappa(z, z)$ – is the diagonal onsite matrix element of the Green function of the considered system. But further we will consider only s-electrons with the same Fermi momentum, for every layer in the first approximation we may take this matrix element as coinciding with its value in the bulk material constituent of the layer. Moreover, we will absorb the real part of the coherent potential into the value of the Fermi energy and take into account explicitly only its imaginary part $\mathrm{Im}\,\Sigma_i$, whose three values $\mathrm{Im}\,\Sigma^\uparrow \equiv \Sigma_1^{\mathrm{b}}$, $\mathrm{Im}\,\Sigma^\downarrow \equiv \Sigma_3^{\mathrm{b}}$ and $\mathrm{Im}\Sigma_{\mathrm{p}} \equiv \Sigma_2^{\mathrm{b}}$ are taken as the parameters of bulk scattering of spin $\uparrow(\downarrow)$ electrons in ferro- and paramagnetic layer ($\Sigma_{\mathrm{p}}^\uparrow = \Sigma_{\mathrm{p}}^\downarrow \equiv \Sigma_2^{\mathrm{b}}$). In the same manner we introduce the spin-dependent coherent potentials $\mathrm{Im}\,\Sigma^\uparrow \equiv \Sigma_1$ and $\mathrm{Im}\,\Sigma^\downarrow \equiv \Sigma_2$ on the interfaces, located at $z = a$ and $z = a + b$. The Green functions $G(z, z')$ are the solutions of the two equations

$$\left(\frac{\partial^2}{\partial z^2} - \kappa^2 + k_{\mathrm{F}}^2 + 2\mathrm{i}\Sigma_i^{\mathrm{b}}(z)\right)G^0(z, z') = \delta(z - z'), \tag{2}$$

$$G(z, z') = G^0(z, z') + G^0(z, a)\Sigma_1 G(a, z') + G^0(z, a + b)\Sigma_2 G(a + b, z'), \tag{3}$$

where we adopted $\hbar = m = 1$, k_{F} the Fermi momentum and wrote down Eq. (3) for spin $\uparrow$ electron and antiparallel orientation of magnetizations in ferromagnetic layers. The solution of Eq. (3) is

$$\begin{aligned} G(z, z') = {} & G^0(z, z') + A_a G^0(z, a)G^0(a, z') + BG^0(z, a)G^0(a + b, z') \\ & + A_b G^0(z, a + b)G^0(a + b, z') + BG^0(z, a + b)G^0(a, z'), \end{aligned} \tag{4}$$

where

$$A_a = \frac{\Sigma_1(1 - G^0(a+b, a+b)\Sigma_2)}{(1 - G^0(a,a)\Sigma_1)(1 - G^0(a+b,a+b)\Sigma_2) - G^0(a+b,a)\Sigma_1\Sigma_2 G^0(a,a+b)},$$

$$B = \frac{\Sigma_1 G^0(a,a+b)\Sigma_2}{(1 - G^0(a,a)\Sigma_1)(1 - G^0(a+b,a+b)\Sigma_2) - G^0(a+b,a)\Sigma_1\Sigma_2 G^0(a,a+b)},$$

$$A_b = \frac{\Sigma_2(1 - G^0(a,a)\Sigma_1)}{(1 - G^0(a,a)\Sigma_1)(1 - G^0(a+b,a+b)\Sigma_2) - G^0(a+b,a)\Sigma_1\Sigma_2 G^0(a,a+b)}. \tag{5}$$

and

$$G^0(z,z') = \frac{1}{2ik_0}\exp\left(i\int_{z<}^{z>} k_i(z'')\,dz''\right), \tag{6}$$

with $k_i = c_i + id_i = \sqrt{k_F^2 - \kappa^2 + i2\Sigma_i^b(z)} \equiv \sqrt{k_F^2 - \kappa^2 + i2k_F/l_i(z)}$, l_i the elastic mean free path in the ith layer, $k_0 = \sqrt{k_F^2 - \kappa^2}$, and $z^{<(>)}$ is the smaller (larger) of z and z'.

To proceed further we have to substitute Eqs. (4)–(6) into Eq. (1) and calculate two-point conductivity $\sigma(z,z')$ for spin-up and spin-down electrons for both parallel and antiparallel alignment of magnetizations in ferromagnetic layers. Then we calculated the current

$$j(z) = \int \sigma(z,z')E(z')\,dz', \tag{7}$$

where $E(z')$ is the effective electrical field, which has to be found from Eq. (7) under constraint that $j(z) \equiv \text{const}$ (the current in case of CPP geometry has to be divergentless). Let us suppose that $E(z) = E_a$ in the left ferromagnetic layer, $E(z) = E_b$ in the spacer and $E(z) = E_c$ in the right ferromagnetic layer, $E(z) = C_1\delta(z-a)$ and $E(z) = C_2\delta(z-a-b)$ on the two interfaces. In this case, the expression for the current, for example in the left layer, is

$$\begin{aligned} j_a = \frac{e^2}{2\pi\hbar}\sum_\kappa \Bigg\{ \frac{2}{d_3}E_a + e^{-2d_3(a-z)}\Bigg[-\frac{1}{d_3}E_a(1 + |U_{aa}|^2) \\ + \frac{1}{d_2}E_b(1 - e^{-2d_2 b})(|U_{ab}|^2 - |\tilde{U}_{ab}|^2) + \frac{1}{d_1}E_c e^{-2d_2 b}|U_{ac}|^2 \\ + C_1(1 - |U_{aa}|^2 + |U_{ab}|^2 - |\tilde{U}_{ab}|^2 e^{-2d_2 b}) \\ + C_2(|U_{ab}|^2 e^{-2d_2 b} - |\tilde{U}_{ab}|^2 + |U_{ac}|^2 e^{-2d_2 b})\Bigg]\Bigg\}, \end{aligned} \tag{8}$$

where

$$U_{aa} = \frac{1}{k_0}(A_a + 2Be^{ik_2 b} + A_b e^{2ik_2 b}),$$

$$U_{ab} = 1 - \frac{i}{k_0}(A_a + Be^{ik_2 b}), \qquad \tilde{U}_{ab} = \frac{1}{k_0}(B + A_b e^{ik_2 b}),$$

$$U_{ac} = 1 - \frac{i}{k_0}(A_a + A_b) - \frac{i}{k_0}B(e^{ik_2 b} + e^{-ik_2 b}). \tag{9}$$

Similar expressions give the currents in the spacer and in the right layer. As it is clear from Eq. (8), to fulfill the condition of nondivergence of the current the first terms (constants) have to be equal in every layer and coefficients at the terms proportional to $e^{-2d_i z}$ have to be equal to zero. Besides, the total potential drop across the system is equal to

$$U = aE_a + bE_b + cE_c + C_1 + C_2. \tag{10}$$

The obtained system of equations for five unknown quantities E_a, E_b, E_c, C_1 and C_2 has solutions which are independent of the value of in-plane electron's momentum κ (as it has to be, if we have inter-channel, not conserving κ scattering), if one does not take into account the oscillation terms due to the interference processes between electron waves, scattered on different interfaces. So we averaged the expressions for the currents over the oscillation with thickness of the spacer b (terms in Eq. (9) containing $e^{ik_2 b}$), omitting the terms, proportional to the small parameter $(k_F b)^{-1}$. In this case, the final expressions for the resistance per 1 cm^2 of the cross section for every direction of spin are

$$R^{\uparrow}_{AP(CPP)} = C^{-1}\left\{\frac{a}{l_3} + \frac{b}{l_2} + \frac{c}{l_1} + \frac{1}{k_F}(\Sigma_1 + \Sigma_2)\right\}, \qquad R^{\downarrow}_{AP(CPP)} = C^{-1}\left\{\frac{a}{l_1} + \frac{b}{l_2} + \frac{c}{l_3} + \frac{1}{k_F}(\Sigma_1 + \Sigma_2)\right\},$$

$$R^{\uparrow}_{PCPP)} = C^{-1}\left\{\frac{a}{l_1} + \frac{b}{l_2} + \frac{c}{l_1} + \frac{1}{k_F}2\Sigma_1\right\}, \qquad R^{\downarrow}_{P(CPP)} = C^{-1}\left\{\frac{a}{l_3} + \frac{b}{l_2} + \frac{c}{l_3} + \frac{1}{k_F}2\Sigma_2\right\}, \tag{11}$$

where $C = e^2 k_F^2/(6\pi^2\hbar)$.

It is important to note that Eq. (11) are valid for weak $(1/k_F)(\Sigma_1 + \Sigma_2) \ll 1$ and strong $(1/k_F)(\Sigma_1 + \Sigma_2) \sim 1$ interfacial scattering. So in case of CPP geometry, the additional renormalization of interfacial scattering amplitude for strong scattering does not occur as it occurs for CIP geometry considered below.

3. Giant magnetoresistance in CIP geometry

The expression for CIP conductivity has the form similar to Eq. (1) with substitution instead of derivatives over z and z' the velocity operator in XY plane. The main difference between CIP and CPP is that current in CIP geometry does depend on the z coordinate, so to obtain the total conductivity in this case we have to average the local conductivity $\sigma(z)$ over the total thickness of the system. The final expressions for the conductivities σ_P and σ_{AP} are

$$\sigma_P = \frac{3}{16}\frac{C}{D}\int_0^1 x\,dx\left\{4k_F(a+c)\left(\frac{l_3}{c_3} + \frac{l_1}{c_1}\right) + \frac{8k_F l_2 b}{c_2}\right.$$

$$-\left[l_1^2(2 - e^{-2d_1 a} - e^{-2d_1 c})\left(1 - |U_1^P|^2 - e^{-2d_2 b}\frac{k_0^4}{\mathrm{Den}_1^P}\right)\right.$$

$$\left.+\, l_3^2(2 - e^{-2d_3 a} - e^{-2d_3 c})\left(1 - |U_2^P|^2 - e^{-2d_2 b}\frac{k_0^4}{\mathrm{Den}_2^P}\right)\right] - 2l_2^2(1 - e^{-2d_2 b})$$

$$\times\left[[(k_0 + \Sigma_1)^4 - \Sigma_1^4 e^{-2d_2 b} - (1 - e^{-2d_2 b})\Sigma_1^2(k_0 + \Sigma_1)^2]\frac{1}{\mathrm{Den}_1^P}\right.$$

$$+ [(k_0 + \Sigma_2)^4 - \Sigma_2^4 e^{-2d_2b} - (1 - e^{-2d_2b})\Sigma_2^2(k_0 + \Sigma_2)^2]\frac{1}{\mathrm{Den}_2^{\mathrm{P}}}\Bigg]$$

$$+ \left[l_1 l_2 (4 - e^{-2d_1a} - e^{-2d_1c})(1 - e^{-2d_2b})((k_0 + \Sigma_1)^2 + \Sigma_1^2 e^{-2d_2b})\frac{k_0^2}{\mathrm{Den}_1^{\mathrm{P}}}\right]$$

$$+ \left[l_2 l_3 (4 - e^{-2d_3a} - e^{-2d_3c})(1 - e^{-2d_2b})((k_0 + \Sigma_2)^2 + \Sigma_2^2 e^{-2d_2b})\frac{k_0^2}{\mathrm{Den}_2^{\mathrm{P}}}\right]\Bigg\}, \tag{12}$$

$$\sigma_{\mathrm{AP}} = \frac{3}{16}\frac{C}{D}\int_0^1 x\,\mathrm{d}x\Bigg\{4k_{\mathrm{F}}(a + c)\left(\frac{l_3}{c_3} + \frac{l_1}{c_1}\right) + \frac{8k_{\mathrm{F}} l_2 b}{c_2}$$
$$- [l_3^2(2 - e^{-2d_3a} - e^{-2d_3c})(1 - |U_1^{\mathrm{AP}}|^2) + l_1^2(2 - e^{-2d_1a} - e^{-2d_1c})(1 - |U_2^{\mathrm{AP}}|^2)]$$
$$- 4l_2^2(1 - e^{-2d_2b})[(k_0 + \Sigma_2)^2(k_0 + \Sigma_1)^2 - \Sigma_2^2\,\Sigma_1^2\,e^{-2d_2b}$$
$$- (\tfrac{1}{2})(1 - e^{-2d_2b})(\Sigma_2^2(k_0 + \Sigma_1)^2 + \Sigma_1^2(k_0 + \Sigma_2)^2)]\frac{1}{\mathrm{Den}^{\mathrm{AP}}}$$
$$+ \left[l_2 l_3 (4 - e^{-2d_3a} - e^{-2d_3c})(1 - e^{-2d_2b})((k_0 + \Sigma_1)^2 + \Sigma_1^2 e^{-2d_2b})\frac{k_0^2}{\mathrm{Den}^{\mathrm{AP}}}\right]$$
$$+ \left[l_2 l_1 (4 - e^{-2d_1a} - e^{-2d_1c})(1 - e^{-2d_2b})((k_0 + \Sigma_2)^2 + \Sigma_2^2 e^{-2d_2b})\frac{k_0^2}{\mathrm{Den}^{\mathrm{AP}}}\right]$$
$$+ \left[l_1 l_3 (4 - e^{-2d_1a} - e^{-2d_1c} - e^{-2d_3a} - e^{-2d_3c})e^{-2d_2b}\frac{k_0^4}{\mathrm{Den}^{\mathrm{AP}}}\right]\Bigg\}, \tag{13}$$

where $c_i + \mathrm{i}d_i = k_{\mathrm{F}}\sqrt{1 - x + \mathrm{i}2/(l_i k_{\mathrm{F}})}$, $k_0 = k_{\mathrm{F}}\sqrt{1 - x}$, $x = \kappa^2/k_{\mathrm{F}}^2$, $D = a + b + c$ and

$$\mathrm{Den}_{1(2)}^{\mathrm{P}} = (k_0 + \Sigma_{1(2)})^4 - \Sigma_{1(2)}^4 e^{-4d_2b}, \qquad \mathrm{Den}^{\mathrm{AP}} = (k_0 + \Sigma_2)^2(k_0 + \Sigma_1)^2 - \Sigma_2^2\Sigma_1^2 e^{-4d_2b},$$

$$|U_{1(2)}^{\mathrm{P}}|^2 = \frac{1}{\mathrm{Den}_{1(2)}^{\mathrm{P}}}\left[\Sigma_{1(2)}^2(k_0 + \Sigma_{1(2)})^2 + \frac{k_0 - \Sigma_{1(2)}}{k_0 + \Sigma_{1(2)}}\Sigma_{1(2)}^2(k_0^2 + \Sigma_{1(2)}^2)e^{-4d_2b}\right],$$

$$|U_{1(2)}^{AP}|^2 = \frac{1}{\mathrm{Den}^{\mathrm{AP}}}\left[\Sigma_{2(1)}^2(k_0 + \Sigma_{1(2)})^2 + \frac{k_0 - \Sigma_{2(1)}}{k_0 + \Sigma_{2(1)}}\Sigma_{1(2)}^2(k_0^2 + \Sigma_{2(1)}^2)e^{-4d_2b}\right].$$

It is clear from Eqs. (12) and (13) that spin-dependent interfacial scattering as well as the bulk gives the contribution to GMR in CIP geometry through the classical size effect. Now it is important to note that the coherent potential $\Sigma_{1(2)}$ of isolated interface is renormalized to $\Sigma_{1(2)}^{\mathrm{eff}} = \Sigma_{1(2)}/(1 + \Sigma_{1(2)}/k_{\mathrm{F}})$. This renormalization has a clean physical interpretation: electron scattering on interface influences the total CIP conductivity, and the contribution of the interface scattering to resistivity reaches the maximum for 'diffuse' scattering. In this regime, the electron forgets its history after scattering on the length $\sim k_{\mathrm{F}}^{-1}$, and this length cannot be shorter for any value of the initial scattering potential $\Sigma_{1(2)}$. The ratio of renormalized interfacial coherent potentials for up and down spin electrons tends to unity with increasing of interfacial scattering. To make this point clear, we plotted in Fig. 1 the dependence of GMR $(\sigma_{\mathrm{P}} - \sigma_{\mathrm{AP}})/\sigma_{\mathrm{P}}$ versus $\lambda_{\mathrm{s}}^{\downarrow}$, where $\lambda_s^{\downarrow(\uparrow)} = k_{\mathrm{F}} a_0/\Sigma_{2(1)}$ is the mean free path due to the scattering of spin-down (up) electrons for fixed $p_{\mathrm{b}} = l_1/l_3 = 5$ and several values of $p_{\mathrm{s}} = \lambda_{\mathrm{s}}^{\uparrow}/\lambda_{\mathrm{s}}^{\downarrow}$. For $p_{\mathrm{s}} > p_{\mathrm{b}}$ this dependence has a maximum. We can explain such behaviour as follows: for large λ_{s}, $p_{\mathrm{s}}^{\mathrm{eff}} = (\lambda_{\mathrm{s}}^{\uparrow}(1 + a_0/\lambda_{\mathrm{s}}^{\uparrow}))/(\lambda_{\mathrm{s}}^{\downarrow}(1 + a_0/\lambda_{\mathrm{s}}^{\downarrow})) \approx p_{\mathrm{s}} > p_{\mathrm{b}}$ so increasing the interfacial scattering gives an additional contribution to the total GMR, but for small λ_{s}, $p_{\mathrm{s}}^{\mathrm{eff}}$ decreases and it may become smaller than p_{b}, therefore, the additional interfacial scattering is less asymmetric in the direction of spin, so the GMR began to

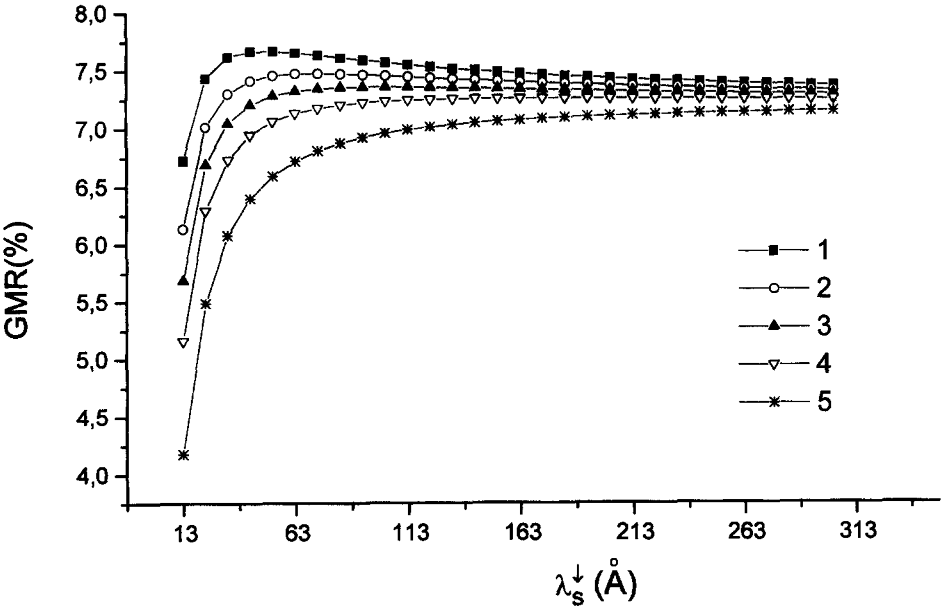

Fig. 1. CIP GMR of sandwiches F 40 Å/P 10 Å /F 40 Å versus min mean free path $\lambda_s^\downarrow$ at interfaces ($\lambda_s^\downarrow$ varying from 13 up to 303 Å). The parameters are $l_1/l_3 = 120$ Å/24 Å; $l_2 = 250$ Å; $k_F = 1$ Å^{-1}; $a_0 = 3$ Å, $\lambda_s^\uparrow/\lambda_s^\downarrow = 20$ – curve 1; $\lambda_s^\uparrow/\lambda_s^\downarrow = 10$ – curve 2; $\lambda_s^\uparrow/\lambda_s^\downarrow = 7$ – curve 3; $\lambda_s^\uparrow/\lambda_s^\downarrow = 5$ – curve 4; $\lambda_s^\uparrow/\lambda_s^\downarrow = 3$ – curve 5.

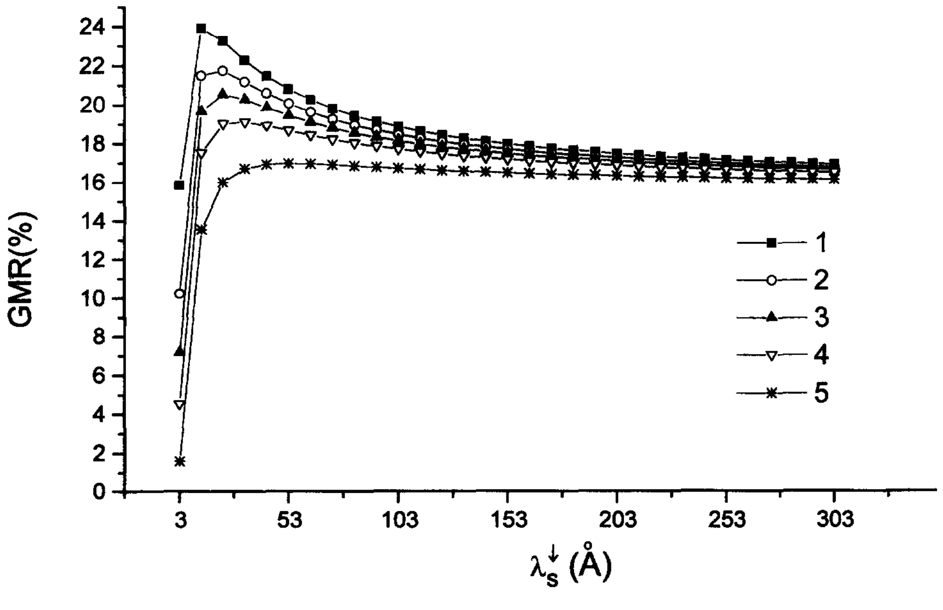

Fig. 2. CIP GMR of multilayer F 40 Å/P 10 Å/F 40 Å /P 10 Å versus min mean free path $\lambda_s^\downarrow$ at interfaces ($\lambda_s^\downarrow$ varying from 3 up to 303 Å). The parameters are $l_1/l_3 = 120$ Å/24 Å; $l_2 = 250$ Å; $k_F = 1$ Å^{-1}; $a_0 = 3$ Å. $\lambda_s^\uparrow/\lambda_s^\downarrow = 20$ – curve 1; $\lambda_s^\uparrow/\lambda_s^\downarrow = 10$ – curve 2; $\lambda_s^\uparrow/\lambda_s^\downarrow = 7$ – curve 3; $\lambda_s^\uparrow/\lambda_s^\downarrow = 5$ – curve 4; $\lambda_s^\uparrow/\lambda_s^\downarrow = 3$ – curve 5.

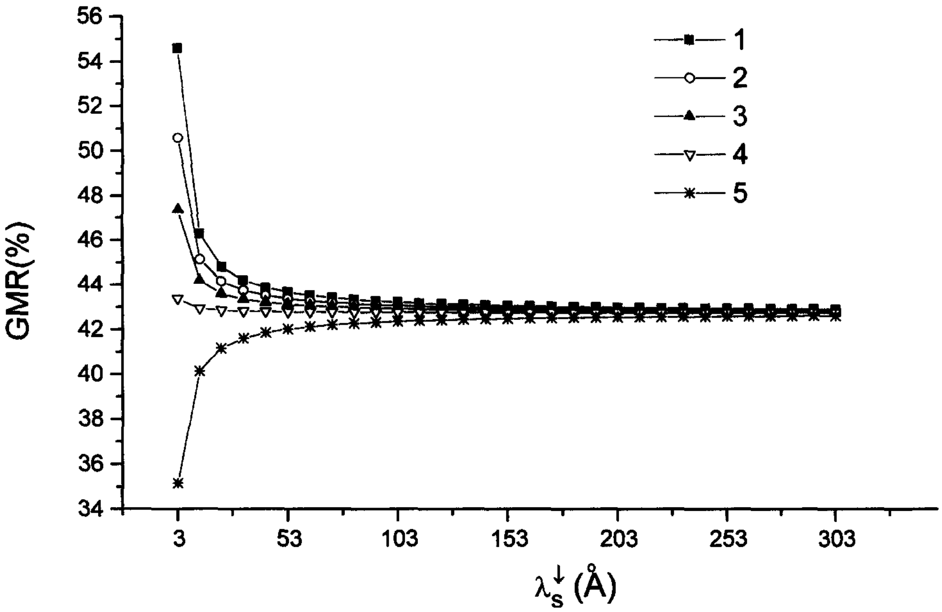

Fig. 3. CPP GMR of sandwiches F 40 Å/P 10 Å/F 40 Å versus min mean free path $\lambda_s^{\downarrow}$ at interfaces ($\lambda_s^{\downarrow}$ varying from 3 up to 303 Å). The parameters are $l_1/l_3 = 120$ Å/24 Å; $l_2 = 250$ Å; $k_F = 1$ Å^{-1}; $a_0 = 3$ Å. $\lambda_s^{\uparrow}/\lambda_s^{\downarrow} = 20$ – curve 1; $\lambda_s^{\uparrow}/\lambda_s^{\downarrow} = 10$ – curve 2; $\lambda_s^{\uparrow}/\lambda_s^{\downarrow} = 7$ – curve 3; $\lambda_s^{\uparrow}/\lambda_s^{\downarrow} = 5$ – curve 4; $\lambda_s^{\uparrow}/\lambda_s^{\downarrow} = 3$ – curve 5.

decrease. Barnas and Bruynseraede [6] investigated the influence of interfacial scattering on CIP GMR and they obtained, for $p_s > p_b$, a monotonic increase of GMR with amplitude of interface roughness. However, since they considered the interfacial scattering only in Born approximation, they missed the effect of renormalization discussed above. In Fig. 2 we plotted the same dependence as in Fig. 1 but for a multilayer with infinite number of periods F/P/F/P. The curves in Figs. 1 and 2 are similar but GMR for an infinite multilayer is larger than for the single sandwich due to repetition of the process. At last, in Fig. 3, we plotted CPP GMR versus $\lambda_s^{\downarrow}$. In this case the curve is monotonic (GMR increases for $p_s > p_b$ and decreases for $p_s < p_b$). But we mentioned earlier that in the expression for CPP GMR appeared only nonrenormalized coherent potentials $\Sigma_{1(2)}$, therefore the maximum on the curve has to be absent. So we came to the conclusion that for large spin-dependent interfacial scattering CPP GMR is larger than CIP GMR, what is always true in experiment. It is interesting to notice that Eq. (11) for CPP resistivities coincide with Eqs. (44), (45) in Ref. [8], if one identifies the phenomenological parameter $r^{\uparrow(\downarrow)}$ (resistivity of interface in Ref. [8]) with $\Sigma_{1(2)}/(k_F C)$. The same values of the interfacial coherent potentials define the CIP conductivities (Eqs. (12) and (13)) (in Ref. [4] the CIP conductivities are defined through phenomenological parameter T, the probability of the electron coherent transmission through the interface, and no connection between parameters T in CIP and r in CPP was established). Finally, we have four parameters l_1, l_3, Σ_1 and Σ_2 defining four measured quantities $\sigma_{AP(CIP)}$, $\sigma_{P(CIP)}$, $R_{AP(CPP)}$ and $R_{P(CPP)}$.

Acknowledgements

This work was supported by the Russian fund for basic research (grant No. 96-02-19681a), INTAS (grant No. 93-0718) and NATO (grant HTECH.LG 951527).

References

[1] M.N. Baibich et al., Phys. Rev. Lett. 61 (1988) 2472.
[2] G. Binash et al., Phys. Rev. B 39 (1989) 4828.
[3] B. Dieny, J. Magn. Magn. Mater. 136 (1994) 335.
[4] A. Barthelemy, A. Fert, Phys. Rev. B 43 (1991) 13124.
[5] A. Vedyayev, B. Dieny, N. Ryzhanova, Europhys. Lett. 19 (1992) 329.
[6] J. Barnas, Y. Bruynseraede, Phys. Rev. B 53 (1996) 5449.
[7] P. Levy, Solid State Physics 47 (1994) 367.
[8] T. Vallet, A. Fert, Phys. Rev. B 48 (1993) 7099.
[9] A. Vedyayev et al., Phys. Lett. A 198 (1995) 267.
[10] C.L. Kane, R.A. Serota, P.A. Lee, Phys. Rev. B 37 (1988) 6701.